DOI: 10.13009/EUCASS2022-6106

Assessment of Electron Transpiration Cooling phenomena in Inductively-Coupled Plasma facility

Victor Lafaurie[⋆†], *Alan Viladegut* [⋆†], *Bernd Helber* [⋆] *and Olivier Chazot* [⋆]
[⋆]*Von Karman Institute For Fluid Dynamics*
Chaussee de Waterloo 72, B-1640 Rhode-Saint-Genese, Belgium
victorlafaurie@yahoo.fr · alan.viladegut@vki.ac.be
[†]Corresponding author

Abstract

The present work aims at assessing how to measure physical quantities that relate to Electron Transpiration Cooling (ETC) phenomena. This is carried out through a test campaign in the Plasmatron facility at the Von Karman Institute, which allows reaching high surface temperatures under flows stagnating on candidate samples. Graphite samples (work function of 4.7 eV) were tested and found to emit currents between 0.05 to 0.1 A when heated with nitrogen plasma flow, seemingly following theoretical predictions for the lower temperature ranges of 2000 to 2250 degrees celsius.

1. Introduction

1.1 Motivation

Hypersonic cruise flight is a technical feat that still needs investigation. While multiple technical demonstrators could reach high Mach numbers, such as the Boeing X-51 Waverider at Mach 5.1, and the NASA X-43 A which flew at Mach 9.64, these only remained in the hypersonic regime for tens of seconds. In order to achieve a fully functioning and prolonged flight, several challenges must be addressed, most critically propulsion and thermal management. The latter issue could be mitigated through Thermal Protection System (TPS) based on Electron Transpiration Cooling (ETC).

1.2 Thermionic Emissions and Electron Transpiration Cooling

Despite ETC being theorised and first developed in the 1960s, little literature can be found on the topic. The works of Uribarri et al[15] and Hanquist et al[6] were especially useful in first understanding the basic working principles of ETC and identifying the main challenges to address the topic. Key texts such as Richardson's[11] and Goebel's[4] were instrumental in an initial review of the fundamental physical principles of thermionic emissions. State of the art material development and their characteristics are provided by Rand[12] and by Yoshizumi.[16] Similarly, exhaustive resources existed regarding computational methods for ETC, as given most notably by Hanquist et al,[6–8] which highlighted the potential efficiency of this thermal management method. Although somewhat more scarce, experimental ETC results also exist, as those performed by Touryan et al,[13,14] which corresponds to a measurement campaign of thermionic emissions in a plasma wind tunnel, to more recent attempts by Chazot et al[2] and Meyers et al,[10] which performed measurements attempting to correlate thermionic emission measurements with cooling at the stagnation point.

The goal of ETC is to remove heat from the leading edge of an hypersonic vehicle by releasing electrons through thermionic emission. Electrons are emitted from the leading edge material surface (or emitter) after acquiring enough energy to overcome its potential barrier, known as the work function, as described by the Richardson-Dushman equation:

$$J = AT^2 \exp\left[-\frac{\Phi \mathrm{e}}{k_B T}\right] \tag{1}$$

Here, J is the current density for emitted electrons, A is a constant, usually assumed to be 120 $\mathrm{Acm^{-2}K^{-2}}$, T is the temperature, Φ_e is the material work function and k_B is the Boltzmann's Constant.

The current densities as a function of temperature for two types of materials: pure materials, such as graphite (Φ = 4.7 eV) and tungsten (Φ = 4.5 eV), or manufactured materials, such as Aluminate Electride (Φ = 0.6 eV)[12] or

DOI: 10.13009/EUCASS2022-6106

Mayenide Electride (Φ = 2.1 eV)[16] are shown in Figure 1. The extreme dependence of thermionic emissions on the work function is evident. The lower the work function, the higher the current density and therefore the more energy can theoretically be removed from the leading edge. In effect, at 2500K, halving of the work function leads to a 10^4 multiplication in the current density, thus showing why research of more efficient materials is key to implement ETC in long hypersonic flights.

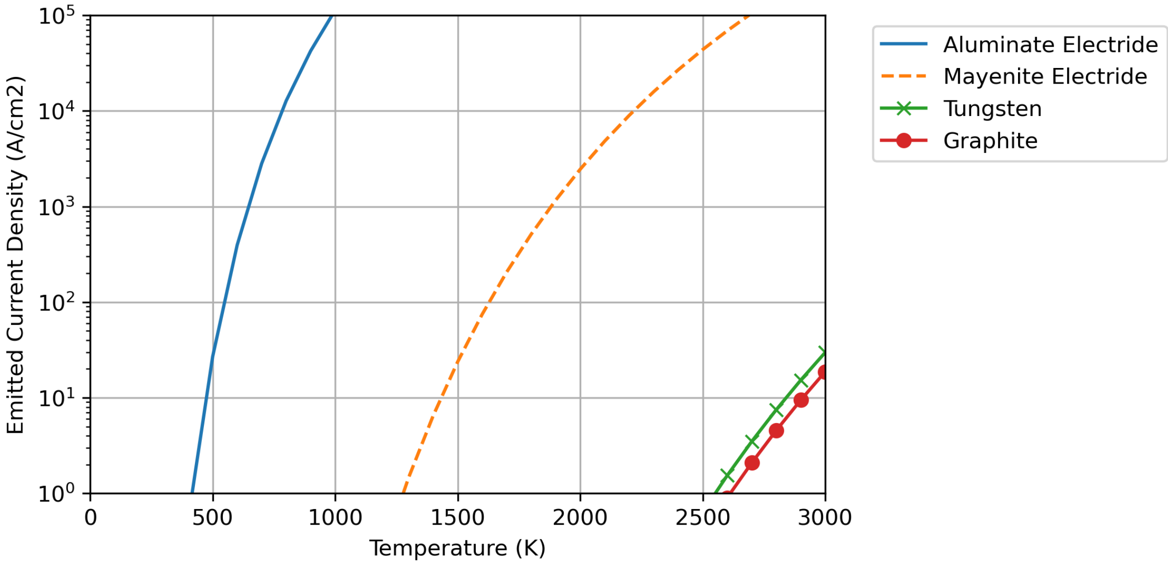

Figure 1: Thermionic emissions as a function of temperature for variety of materials

In practice, material work function is far from being the only consideration in ETC. The fact is, high emissions of electrons can lead to space charge distributions around the material sample, which can limit the effectiveness of ETC. One way to overcome this issue consists of removing the space charge by closing the electric circuit between the vehicle and the gas, thus developing a plasma sheath around the wall of the vehicle. This sheath is characterised by a layer of excess positive charge near the wall to balance the material surface's negative charge as explained by Gangemi .[3]

To close the ETC circuits, the emitted electrons at the stagnation point flow downstream and reattach further, on the area referred to as the collector, as shown in Figure 2. The mechanisms for this transport are either natural, by travelling in the plasma sheath, or by addition of a potential difference between emitter and collector to overcome the sheath potential that is formed. By reattaching to the colder collector, the energy removed from the leading edge is spread on a much larger area, ensuring the materials remain within their operational temperature limit everywhere. These electrons then need to be recirculated back to the leading edge so as not to create a charge accumulation at the collector, which would prohibit electrons from leaving the emitter or be bounced back to the emitting surface.

Finally, an electrical insulator is required between collector and emitter for proper function of ETC. Various materials have been considered for this purpose, the key parameter being electrical resistivity at very high temperatures. In the course of this project, Alumina and Silicon Carbide were considered, as found by Gomi[5] and Auerkari.[1]

In order to ensure electron transpiration cooling as an efficient method of thermal management, several criteria can be identified. Uribarri et al[15] put forward several such parameters to measure the efficacy of ETC, two of which will be discussed here.

Firstly, a comparison between radiated heat flux from the surface and heat removed by ETC, where the former is measured using Stefan Boltzmann's law $P_{rad} = \sigma T^4$ assuming black body radiation (emissivity of 1), with $\sigma = 5.67 \times 10^-8$ WK^{4}m^{-2}; and the total power carried away by ETC per unit area, estimated as:

$$P_{ETC} = J\frac{\Phi_e}{Qe}1.6 \times 10^{-19}, \tag{2}$$

with Qe being the elementary charge. Taking the ratio of these expressions, one can obtain:

$$\gamma_{rad} = 2 \times 10^{13}\frac{\Phi_e}{T^2}\exp{(-\frac{\Phi_e}{T})} \tag{3}$$

This ratio can then be used to identify the temperature at which ETC becomes more effective at removing heat from the leading edge than radiation for a given work function, that is, when $\gamma > 1$. As shown in Figure 3, ETC

DOI: 10.13009/EUCASS2022-6106

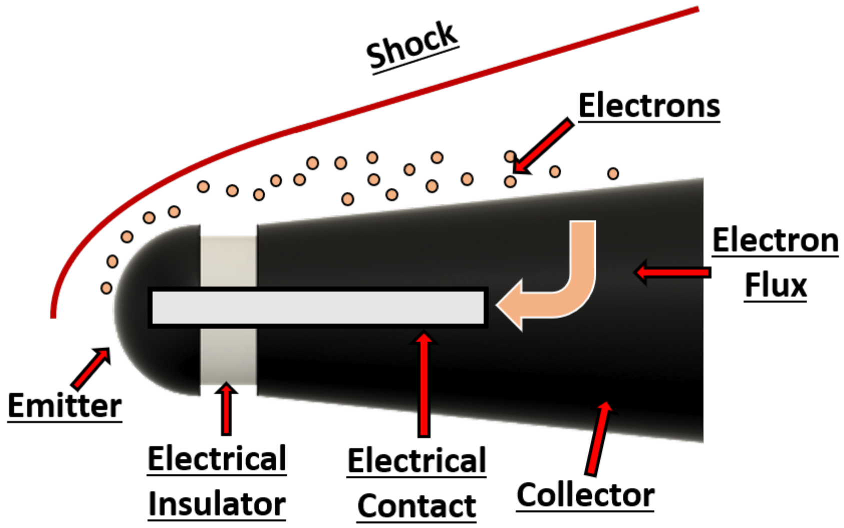

Figure 2: General diagram of Electron Transpiration Cooling

quickly overtakes radiative cooling for all four materials previously considered. Finally, it is important to note that in reality, the effects of these two methods of cooling would be compounded, meaning graphite at 1750 K would theoretically have twice as much cooling in an ETC configuration as it would with only radiative cooling. This is of course a simplification as many effects have been neglected for the purposes of this demonstration, but serves as a good illustration to the potential of ETC.

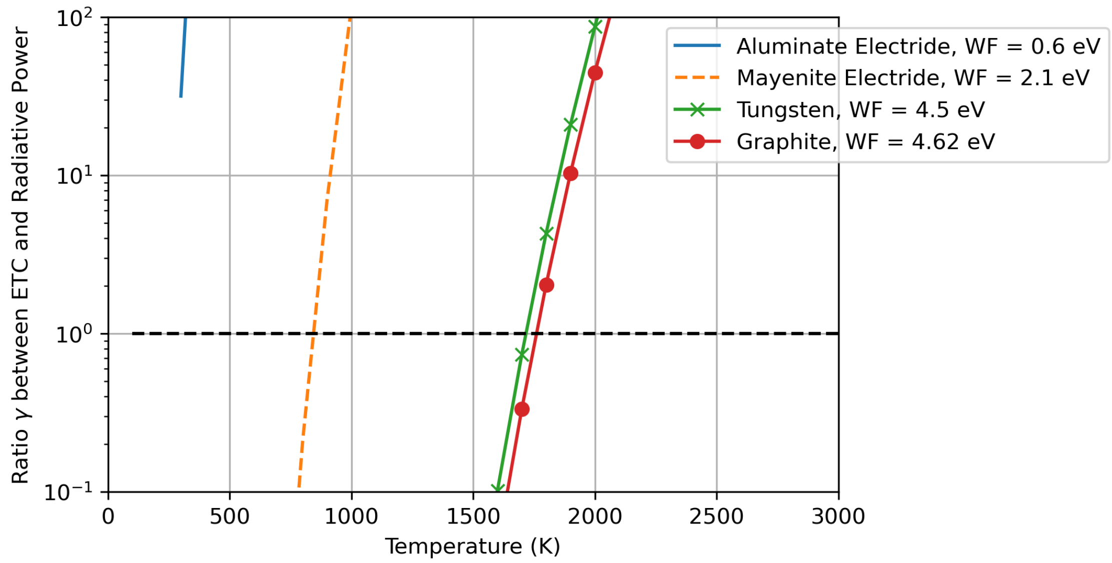

Figure 3: Ratio of ETC to Radiative cooling power

The second method of checking effectiveness of ETC comes from measuring heating of the rod used to recirculate electrons from collector to emitter. In effect, the large current being emitted needs to be equal to that in the rod, which may lead to resistive effects and Joules heating. A parameter to study this effect is proposed as follows:

$$\alpha = \frac{\dot{q}_{ETC} A}{\dot{q}_J V} = \frac{J\phi A}{\rho J^2 A l} = \frac{\phi}{\rho J l} = \frac{\phi}{\left(\frac{\rho l}{A}\right) I} = \frac{\phi}{RI} \tag{4}$$

where I = JA and ρ is the resistivity and assuming (l/A) is of order 10. From,[15] it is expected that values of resistivity higher than 10^{-5} Ωm should lead to α values much larger than 1 for currents of the order of kA. This

DOI: 10.13009/EUCASS2022-6106

effectively means that the heat removed from the leading edge will be much higher than the heat generated from resistivity effects in the connecting rod and will not lead to excessive heating of the inside of the wing leading edge.

So far, the emitter current has been assumed to be of the same order of that dictated by the Richardson-Dushman equation. However, limitations can occur in the form of retarding electric fields caused by the electrons' own space charge. This becomes an additional potential barrier which the electrons need to overcome in order to separate from the surface, which can reduce the cooling efficiency of ETC drastically. The appearance of space-charge is one of the most critical issues to the full implementation of ETC in real flight.

2. Test Campaign

A test campaign aiming at the observation of ETC on hot surfaces with low work functions is performed in the VKI Plasmatron facility. For that, a new probe is conceived with two thermionic surfaces: one emitter and one collector, connected through a resistor to measure electric current between them.

2.1 Probe Design

Proper design of the geometry of the probe is of great importance in order to maximise the current and therefore the cooling effect by ETC. However, there is little experimental data available regarding the shapes and size to achieve this. Turning once again to Touryan,[13,14] two parameters were highlighted that impacted the power generation and their ideal values were presented. Theses values are shown in Table 1.

The first parameter shown to impact power generation was the emitter to collector area ratio $\beta = A_e/A_c$. Experimental results obtained by Touryan et al indicated a higher current for a smaller β. This has led the decision for this project of a ratio between 0.1 and 0.15.

The second parameter driving the probe geometric design was the angle of the conical collector. The optimal values shown in Table 1 were found from the optimal results obtained in the experimental campaign, also from Touryan et al.[13]

Table 1: Optimal Geometric Values from Touryan et al[13]

Parameter	Optimum range
β	≤ 0.15
Collector Body Angle	6 to 10 °

Having identified the key geometric parameters, the design of the ETC probe was therefore entirely constrained by the emitter area, the β value and the collector angle. The layout and axisymmetric nature of the probe were inspired both by Touryan's highest performing probes[13] and a theoretical design from the previous ETC campaign at the VKI.[2]

For the test campaign of this work, the emitter was chosen to be a half-hemispherical body with a diameter of 30 mm. This geometry, smaller than what was previously tested in the Plasmatron for ETC (50 mm diameter in 2017[2]) was selected to enable a higher heat-flux and therefore faster heating of the test sample to reach emissive values. This would also allow to change the leading edge temperature more easily in order to modulate and see if the current changed. For a probe made of graphite, a theoretical current of 1 A should be achievable at 2400 K according to Richardson-Dushman's equation (Equation 1).

Along with the emitter, two different collectors were manufactured out of graphite, their geometrical properties are given in Table 2.

Table 2: Probe Collector Properties

Model	β	Cone Angle
Collector 1	0.1371	7 degrees
Collector 2	0.127	9 degrees

Electrical contact inside the probe between emitter and collector was ensured by a tungsten rod, while electrical insulation between emitter and collector's external surfaces was done using cylinders of alumina. The thickness of said cylinders was to be changed to study the impact of the distance between emitter and collector on the emissions. A sectional view of one of the probes can be found in Figure 4.

DOI: 10.13009/EUCASS2022-6106

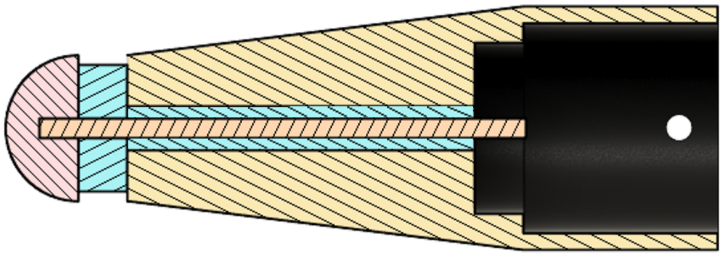

Figure 4: Sectional view of the design for the 7 degree collector. Emitter is pink, collector is yellow, alumina insulators are blue and tungsten rod is orange.

2.2 Test Facility

The Plasmatron facility at the VKI is a high enthalpy plasma wind tunnel typically used for reproduction of re-entry atmospheric plasma and aerothermodynamic testing. The plasma is generated by heating the gas with electrical current loops induced by an electromagnetic field. This type of plasma generation, referred to as inductively-coupled plasma, is typically of higher purity than classical arc-jets, thanks to the lack of pollution originated from electrode erosion. The torch is powered by a high voltage, high power and high frequency generator (2 kV, 1.2 MW, 400 kHz), allowing to generate heat fluxes in excess of 5 MW/m2 when a converging nozzle is mounted, as done in the present campaign.

Here, Nitrogen was used in order to prevent graphite from oxidising at high temperatures. Furthermore, its lower electron density content (with respect to air plasma) should theoretically facilitate measurement of the thermionic emissions.

2.3 Measurement and Data Acquisition

The main objective of this study is to measure the current between emitter and collector, and correlate this with the temperature at the leading edge of the probe. To this end, a simple circuit was developed including a known resistance of 9.5 Ω. The potential drop measured across this resistance is recorded, and the current can be recovered with Ohm's law. As current is constant through a circuit in series, the current passing through a known resistance should theoretically be the same as the current that travels through the plasma. A schematic of the proposed circuit is shown in Figure 5.

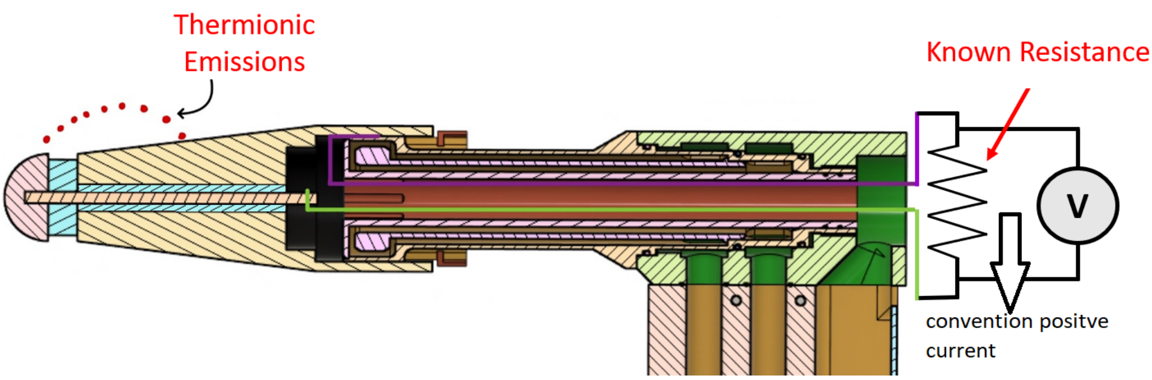

Figure 5: Sectional view of the model and the circuit envisioned to measure the current.

Note should be made that this Figure 5 is only a representation of the circuit and certain aspects, specifically the cable placements and the circuit configuration were varied during the campaign. Also, a switch was added next to the known resistance.

In addition to the current, temperature measurements were performed over the model. Stagnation point temperature was measured using a Raytek MR1S 2-color pyrometer, while recordings on the collector were performed using and infrared camera with assume emissivity of 0.85. Finally, two Type-E thermocouples were placed by the tungsten rod and at the very back of the collector to record the temperature at the points of electrical contact within the probe.

DOI: 10.13009/EUCASS2022-6106

3. Test Configurations and Results

This experimental campaign had several objectives that required varying arrangements of the probe and its circuit. These are found in Table 3.

Table 3: Goals of the test campaign

Primary Goal	Correlation found between measured current and thermionic emissions
Secondary Goal	Correlation found between current and temperature drop
Tertiary Goal	Correlation found between temperature drop and imposed potential difference

In order to test for the initial goal, the circuit as shown in Figure 5 is a good baseline. However, despite the low electron density in nitrogen plasma, there remains the possibility that the plasma around the probe becomes electrically conductive, thus influencing the measurement of current. To better interpret this data, two other structures were proposed. Firstly, the choice was made to perform the same measurements as the baseline configuration, but successively grounding the emitter and the collector. A description of these set-ups can be found in Figure 6

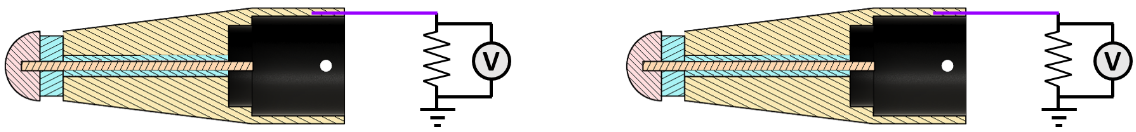

(a) Grounded collector (b) Grounded emitter

Figure 6: Grounded configurations

For all results presented, the procedure remained the same. The probe was press-fitted onto the water-cooled probe holder available on top of the Plasmatron chamber. The holder was wrapped with Kapton tape to avoid electric conductivity between the collector and the holder. This ensured the both emitter and collector to float with the plasma potential, which remains unknown. Vacuum was made and the plasma jet was fitted with a supersonic converging nozzle. The distance between tip of the probe and nozzle exit was 7.5 cm. This was done to increase the heating rate on the emitter relative to the collector. Each probe was lowered into the plasma jet from its position above and the point of complete immersion has been clearly indicated in the results to assess any transient phenomena. After a set amount of exposure time, the plasma was switched off and nitrogen was blown on the model to cool it down. An image of the probe inside of the chamber can be found in Figure 7.

Figure 7: ETC probe with Collector 2

3.1 Baseline Results

Baseline testing was performed with both the collector geometries in the manner described previously and the results are shown in Figure 8. Over all 4 runs performed (2 for each collector), the behaviour observed in the measured current is similar. An initial spike appears while the probe is lowered in the plasma, and an initial decrease is then followed by

DOI: 10.13009/EUCASS2022-6106

an increase in the current which seems to follow the same trend as the stagnation temperature, in line with thermionic emission theory. Finally, the current abruptly returns to 0 when the plasma is switched off.

Notice that testing occurs for an average duration of 30 to 40 seconds. This was done intentionally, as any further testing consistently lead to the wires used to measure the current melting, despite the base of the probe being water cooled.

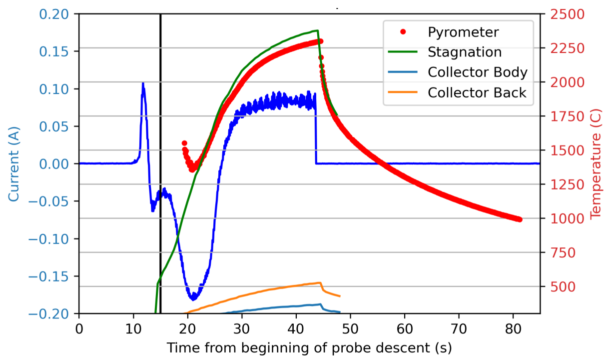

(a) Collector 1, 600 kW: test 1

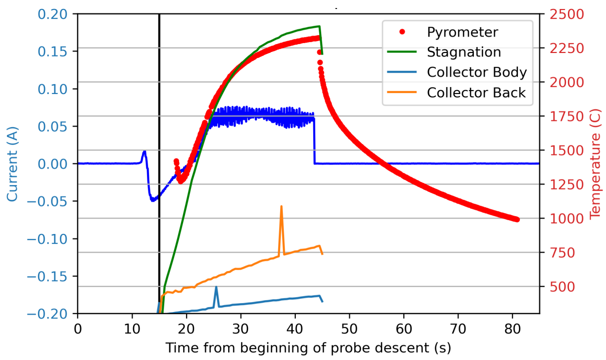

(b) Collector 1, 600 kW: test 2

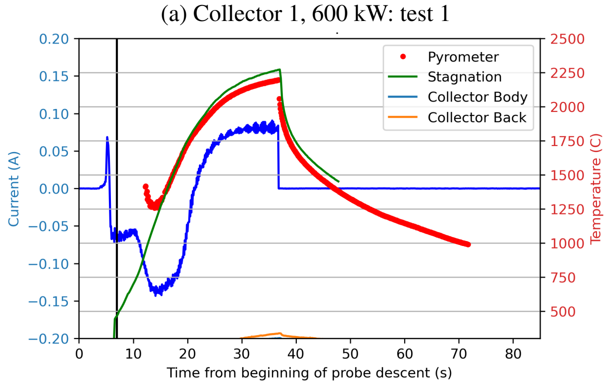

(c) Collector 2, 600 kW: test 1

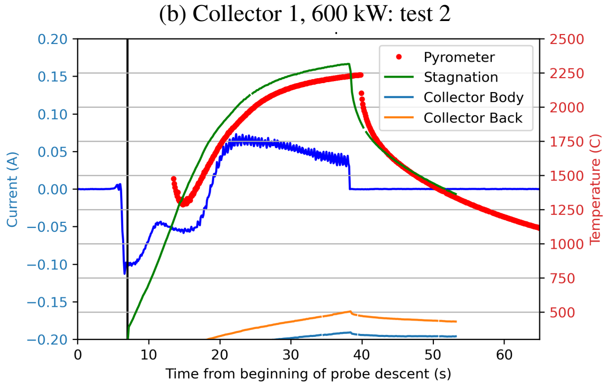

(d) Collector 2, 650 kW: test 2

Figure 8: Measured currents and temperatures for both collector configurations

The current behaviour around the time of insertion of the probe into the plasma can be explained by the notion that the probe is mechanically lowered into the flow. In that sense, as the collector is wider than the emitter, it is the first probe surface to come into contact with the plasma. This likely leads to the initial spike, seen with varying intensities in all four tests. This spike might be related to the fact that the collector is set to an electric potential due to the plasma, thus attracting electrons into the system and passing through the resistor (positive signal). As the probe is further lowered, the emitter is also exposed to the plasma. The decrease which follows the full insertion can be explained by the fact that the emitter is set to an electric potential that is higher than that of the collector, thus attracting more electrons and leading to a negative signal. Finally, when the emitter's surface becomes hotter in time, the current trend inverts, and a positive signal is achieved before quickly reaching a plateau, following the theoretical model of thermionic emission.

Unfortunately, the current behavior cannot be related to an actual temperature drop at the stagnation point, making more difficult the assessment of the secondary goal defined in Table 3.

One important point of note from the experiments was the formation of a dark grey layer on the graphite after each run. As observed in Figure 9, sanding down of the probe after experiments removed the blackened layer and revealed the original colour of the graphite. This may be what caused the reduction of current amplitude between the first and second runs on both probes, although the emitter was filed with sandpaper between both runs.

3.2 Grounded Results

Before diving into the specifics of explaining whether the observations made previously corresponded to ETC, it is important to have a look at the grounded configurations of the experiments to provide a good basis for comparison. As explained previously, over the course of two consecutive runs, the emitter and the collector were successively grounded. The results of the current profiles can be found in Figure 10. These configurations provide very similar

DOI: 10.13009/EUCASS2022-6106

Figure 9: 9 degree collector mounted in the Plasmatron.

results to the previous ones, although with more attenuated signals and with a notable spike switch when the collector is grounded. This attenuation could indicate that ETC was observed. Indeed, when the collector is grounded, electrons from the emitter would not travel back to the leading edge throught the Tungsten rod, causing space charge limitations. Conversely, if the emitter is grounded, any emitted electrons would go straight to ground and the collector would become charged quite fast.

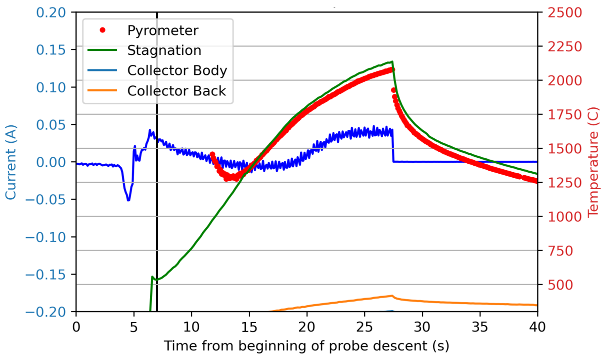

(a) Grounded collector

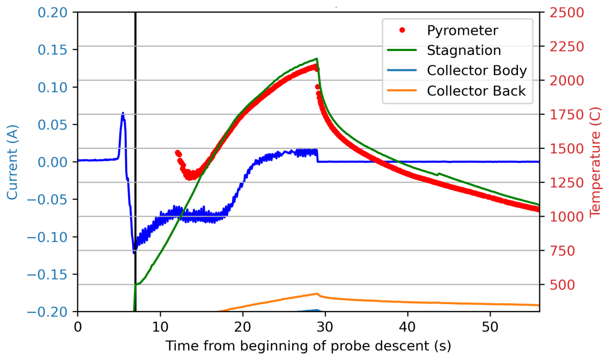

(b) Grounded emitter

Figure 10: Collector 2, 600 kW: current and temperatures for grounded configurations

Temperatures reached in the grounded configurations led to a temperature decrease of around 100 K ($\approx$5%) when compared to the previous setup, and no a remarkable difference is observed between grounded collector and grounded emitter configurations. Therefore, and related to the tertiary goal in Table 3, temperature control remains limited through the change of electric potential on the probe surfaces.

4. Discussion

While repeatability is key in any measurement campaign, the general repeated trend of the current measurements does not conclusively show that ETC was measured. To study this, the measured current was overlaid with the thermionic emissions current, as predicted by the Richardson-Dushman equation.[11] This value was applied a small correction from Touryan,[14] meaning the theoretical maximum current plotted here was:

$$A_{max} = J/\beta \tag{5}$$

The emissions were calculated on the pyrometer data for the stagnation temperature. These results are shown in Figure 11 for all tests in the baseline configuration. Before analysing the data, note that the y-axis does not have the same limits for all four plots, they were plotted on their own scales to facilitate visualisation.

The first thing to note is the visible overlap of the theoretical and measured currents on the portion of plots where the experimental current goes from negative to positive. This overlap disappears as the experimental current plateaus and the theoretical maximum keeps increasing exponentially.

Focusing now on the plateau, a hypothesis was made that nitridation of the graphite occurred during testing. This nitride layer may have changed the work function of the graphite, which, along with possible space charging of the

DOI: 10.13009/EUCASS2022-6106

probe, limited the possible emissions. These two parameters could well prove to be the main challenges in observing ETC in the baseline configuration. Looking at the grounded part of Figure 11 yields another set of interesting results. Indeed, one can clearly see that the emitter reaches a value around 0 net current when grounded, whereas the collector reaches a values of 0.04 Amps and seems to accurately match the thermionic emission predictions, indicating that perhaps the increased current on the collector is due to the electrons from emitter thermionic emissions. This result should however be nuanced, as the much larger area of the collector means it would by definition see much more electrons from the plasma. As testing was not done with a non-emissive leading edge, it cannot be conclusively said that the measurements correspond to graphite emissions.

5. Conclusion

In the course of this project, a methodology for testing the concept of Electron Transpiration Cooling was developed. This methodology, heavily influenced by past works from Touryan,[14] Chazot[2] and Meyers[9, 10] led to the development of 2 probes to study the key parameters identified for ETC, namely leading edge temperature, area ratio between emitter and collector and collector angle. The key steps for characterising ETC were described as: (i) measurement of a current correlated with thermionic emissions; (ii) correlation of said current with leading edge temperature; and (iii) control of this leading edge temperature with imposition of potential differences, either at the emitter or at the collector. The recorded data seems to indicate that there could be a correlation between measured current and thermionic emissions because observations follow similar trend than the theory. Steady state values, however, seem to reach a limit that are far from those predicted by the model.This could be caused by space-charging effects and chemical reactions between the plasma and the graphite samples.

While remaining on a similar experimental set-up to the one used in this project, one should strongly consider configuration where a potential is imposed between emitter and collector. This would allow to test the limits of Electron Transpiration Cooling, by artificially increasing the current. This should then be correlated with emitter temperature. Similarly, a better characterisation of the probe thermal behaviour would be required, especially around the back part of the emitter. This could be achieved by performing further tests with thermocouples combined with thermal model of the probe. Finally, a slight modification could be envisioned by using a longer tungsten rod to prevent copper cables from melting, thus extending the test times.

A more radical and likely necessary step would also be to change the emitter material. Ideally, the reference sample should have the same thermal, chemical and emissive properties as graphite, but with a much higher work function. Hence, one could isolate the effect of ETC on graphite by comparing the with a reference material not subject to thermionic emissions. Alternatively, using a lower work function material would allow for longer test times due to operating at lower temperature and therefore permit a more thorough parametric study, which will be imperative for the validation of the second and third goals (Table 3) defined in this work.

DOI: 10.13009/EUCASS2022-6106

References

[1] Pertti Auerkari. Mechanical and physical properties of engineering alumina ceramics. *VTT Tiedotteita - Valtion Teknillinen Tutkimuskeskus*, 1996.

[2] Olivier Chazot and B Helber. Plasma wind tunnel testing of electron transpiration cooling concept. Technical report, INSTITUT VON KARMAN DE DYNAMIQUE DES FLUIDES VZW SINT-GENESIUS-RODE Belgium, 2017.

[3] G.M. Gangemi. Development of a fluid solver for air plasma sheath, 2020.

[4] Dan M. Goebel and Ira Katz. Fundamentals of Electric Propulsion: Ion and Hall Thrusters. *Fundamentals of Electric Propulsion: Ion and Hall Thrusters*, pages 1–507, 2008.

[5] Takenori GOMI, Noriyuki FUKUSHIMA, and Junichi MATSUSHITA. High temperature electrical conductivity of b4c, sic and sib6 sintered bodies. *Journal of Advanced Science*, 13(1-2):15–16, 2001.

[6] Kyle M. Hanquist. Modeling of electron transpiration cooling for leading edges of hypersonic vehicles. Technical report, University of Michigan, 2017.

[7] Kyle M. Hanquist, Hicham Alkandry, and Iain D. Boyd. Evaluation of computational modeling of electron transpiration cooling at high enthalpies. *Journal of Thermophysics and Heat Transfer*, 31(2):283–293, 2017.

[8] Kyle M. Hanquist and Iain D. Boyd. Plasma assisted cooling of hot surfaces on hypersonic vehicles. *Frontiers in Physics*, 7(FEB):1–13, 2019.

[9] J M Meyers. Advanced Thermal Protection Systems. Technical report, University of Vermont, 2015.

[10] A. J. Morin, R. Osborn, J. C. Schindler, B. Voll, P. Jagun, D. G. Fletcher, and J. M. Meyers. Inductively coupled facility qualification for electron transpiration cooling investigations. *AIAA Scitech 2020 Forum*, 1 PartF(January), 2020.

[11] O.W. Richardson. The Emission of electricity from hot bodies, 1916.

[12] Lauren P. Rand and John D. Williams. A calcium aluminate electride hollow cathode. *IEEE Transactions on Plasma Science*, 43(1):190–194, 2015.

[13] K. J. Touryan. A hypersonic plasma power generator I. *AIAA Journal*, 3(4):652–659, 1965.

[14] K. J. Touryan. A hypersonic plasma power generator II. Technical report, Sandia Corportation, Albaquerque, 1965.

[15] Luke A. Uribarri and Edward H. Allen. Electron transpiration cooling for hot aerospace surfaces. *20th AIAA International Space Planes and Hypersonic Systems and Technologies Conference, 2015*, pages 1–11, 2015.

[16] Toshihiro Yoshizumi and Katsuro Hayashi. Thermionic electron emission from a mayenite electride-metallic titanium composite cathode. *Applied Physics Express*, 6(1), 2013.

DOI: 10.13009/EUCASS2022-6106

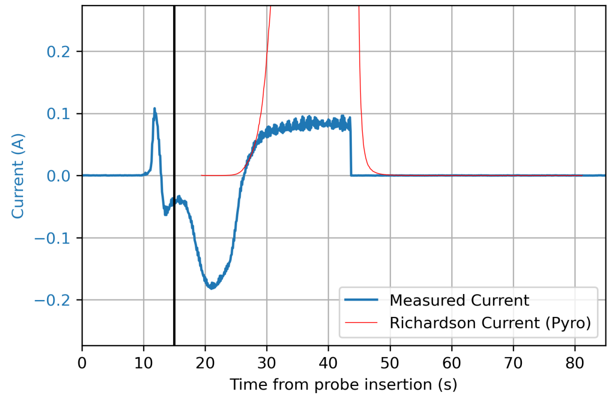

(a) Collector 1, 600 kW: test 1

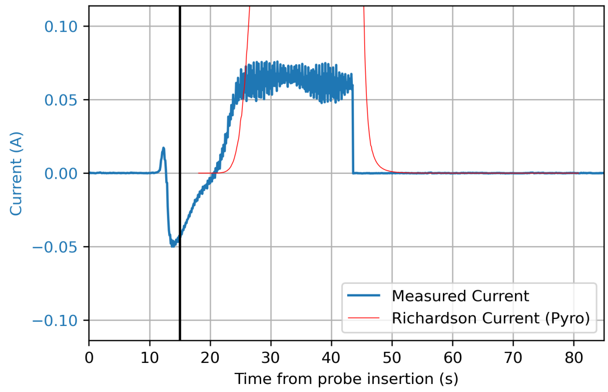

(b) Collector 1, 600 kW: test 2

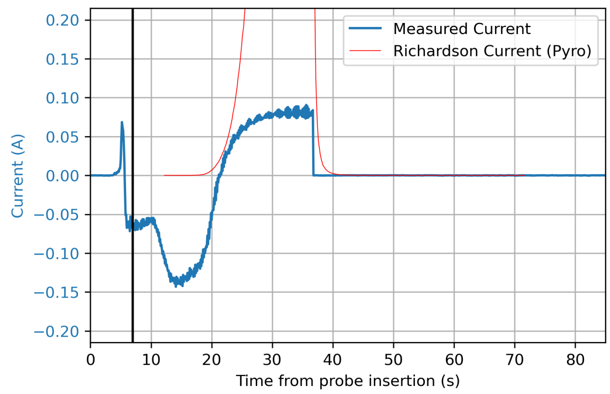

(c) Collector 2, 600 kW: test 1

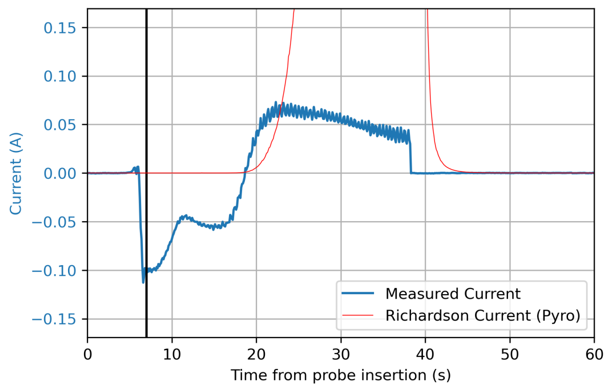

(d) Collector 2, 650 kW: test 2

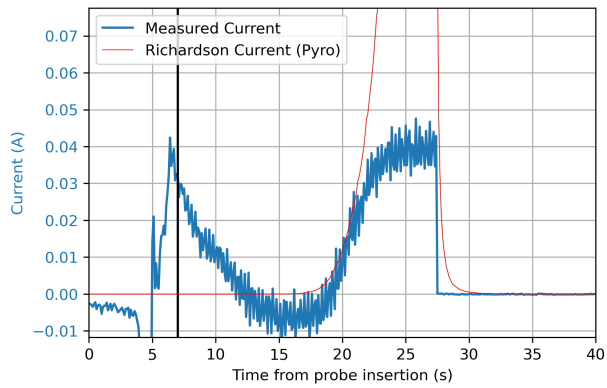

(e) Collector 2, 600 kW: grounded collector

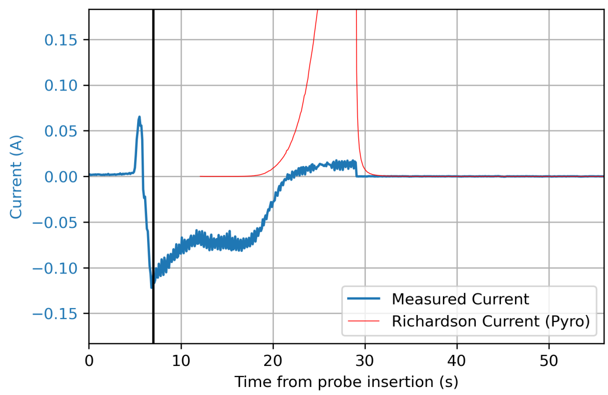

(f) Collector 2, 600 kW: grounded emitter

Figure 11: Comparison of measured currents with thermionic emission model